Hindawi
Advances in Civil Engineering
Volume 2019, Article ID 1732572, 12 pages
https://doi.org/10.1155/2019/1732572

Research Article

Fire Model Test on Temperature Field in the Rescue Station of an Extralong Railway Tunnel

Yanhua Zeng, Kelin Liu, Yong Fang, Xianfu Zhang, and Yun Bai

Key Laboratory of Transportation Tunnel Engineering, Ministry of Education, Southwest Jiaotong University, Chengdu 610031, China

Correspondence should be addressed to Yong Fang; fy980220@swjtu.cn

Received 20 August 2018; Revised 30 October 2018; Accepted 5 December 2018; Published 3 January 2019

Guest Editor: Jian Sun

A rescue station is necessary for an extralong railway tunnel, whose length is generally greater than 20 km. In the rescue station, passenger evacuation, fire fighting, and protection of passengers are organized. It is important to discover the temperature distribution in a rescue station where a train is on fire. This paper performs a similarity simulation model test at 1 : 10 geometric scale to investigate the temperature field in a rescue station. A gasoline pool fire was used as the fire source. The influences of the fire source position and ventilation condition on the temperature field were studied. The results show that (a) the temperature distribution along the tunnel is stable without ventilation, the temperature is lowest when the fire occurs 50 m from the entrance; (b) the fresh air stirred up by fans promotes burning and increases the temperature; (c) the chimney effect causes the temperature field to skew in an uphill direction; (d) the opening of both fans in the adit makes the high-temperature zone to connect through; and (e) the temperature increase at the rescue station can be divided into four stages, and the response of different fire source positions to the opening of fans is not consistent. These findings provide a basis for personnel escape design and a foundation for further study of temperature distribution in a tunnel with a rescue station.

1. Introduction

Fire is always the greatest threat to the operation of a long railway tunnel as it produces a high temperature, toxic fumes, and hot smoke. To reduce the risk of tunnel fire, a rescue station is necessary for an extralong railway tunnel, such as the Lötschberg Base Tunnel (34.6 km) and the Gotthard Base Tunnel (57 km) in Switzerland, the Seikan Tunnel (53.85 km) in Japan, the Channel Tunnel (38 km) in the UK, and the Taihangshan Tunnel (27.8 km) and the Wushaoling Tunnel (20 km) in China [1–4]. In the rescue station, passenger evacuation, fire fighting, and protection of passengers are organized. Tarada et al. [5] reviewed the design of the ventilation and risk control systems and proposed that fire fighting and evacuation are especially vital during the operation of a railway tunnel with a rescue station. Kim and Park [6] investigated the relationship between the ventilation system and escape routes of a rescue station in a very long railway tunnel in Korea by using reduced-scale experiments.

Many studies on fire in a tunnel or underground space have been carried out. Kurioka et al. [7] proposed an empirical equation to predict the maximum temperature of the smoke layer under a tunnel ceiling. Wang et al. [8] proposed a theoretical model using dimensional analysis that could better predict the heat of smoke in a tunnel with vertical shafts. Li et al. [9] found through theoretical deduction that the maximum excess gas temperature beneath the ceiling could be divided into two regions with different ventilation velocity. Li and Ingason [10] also confirmed that these empirical formulae can be applied in the case of a large tunnel fire. Kashef et al. [11] took a new approach in studying ceiling temperature distribution in tunnel fires with natural ventilation by conceptually dividing the tunnel into two fire zones. Wang et al. [12–14] and Ren et al. [15, 16] conducted a series of tests and numerical studies on the fire smoke and the maximum temperature in curved tunnels, together with various fire locations. They found the smoke movement and the maximum temperature to be strongly dependent on the fire location and obviously different from

the straight tunnel fire in curved tunnel fires. Zhang et al. [17] revealed that the utilization of natural wind in the vertical shaft of a super-long highway tunnel can save energy obviously.

Many prototype experiments and field tests have been carried out as well. Yan et al. [18] revealed that the heat transfer on the tunnel liner affects the air temperature in the tunnel greatly without the heat-insulating layer on the liner surface. Hu et al. [19] used full-scale burning tests to test the Kurioka formula and verified the theoretical formula of the maximum temperature under the tunnel ceiling. Ji et al. [20] investigated the influences of different transverse fire locations on the maximum smoke temperature under the tunnel ceiling. In a field investigation, Hu et al. [21] found that the gas temperature decays faster along the ceiling for tunnels with a steeper slope. In the case of twin tunnels, Fang et al. [22] found that there is a "dead zone" ahead of the cross aisle which has a much lower air velocity than in other parts and where hazardous gases are more concentrated and uniformly distributed.

Reduced-scale model experiment has been another popular method in the study of tunnel fires owing to its convenience, ease of control, low cost, and other advantages. Nyman and Ingason [23] performed two reduced-scale tests to explore new correlations between temperature stratification and the Froude number in a tunnel. Fumiaki et al. [24] used a 1/12 scale model tunnel to obtain the temperature characteristics of natural ventilation during smoke extraction in a road tunnel with roof openings. Chow et al. [25] used a reduced-scale experiment to analyze the temperature distribution in an inclined tunnel and found that it was not symmetrically distributed along the sides of the fire. Wang et al. [26] proposed a theoretical model to predict the maximum temperature beneath the ceiling in a tunnel with vertical shafts and compared the calculation results with experimental data.

However, the previous research mainly focused on the maximum temperature under the tunnel ceiling in an ordinary single-tube tunnel. There is no research on the temperature-field distribution of the rescue station. A rescue station is important for personnel evacuation in an extralong railway tunnel (Figure 1), and the temperature-field distribution there is a key concern in personnel evacuation. In this study, a reduced-scale model based on the Gaoligongshan Tunnel was used to investigate the temperature field in the rescue station where a train stopped for rescue in the case of a fire. The results have great significance for the design of rescue stations and evacuation plans for extralong railway tunnels.

2. Model Test

Similarity theory is an important theoretical foundation for a fluid mechanics model experiment. When simulating liquid flow with a free surface, the Froude number is the similarity criterion that must be considered. Based on the results of many verified model experiments, the Froude scaling law is a reliable norm for a model experiment. The model experiment described below is conducted based on Froude scaling.

2.1. Similarity Scale. The results of a model experiment can be considered reliable only if similarity theories which have a significant impact on the model experiment are considered. For this study, a 1 : 10 reduced-scale model was built considering the most important terms and the widely used Froude scaling law. The model included a tunnel, a parallel adit, and nine transverse alleyways. In Froude modeling, the Froude number (i.e., the ratio of inertial force to gravitational force) is determined as follows [27]:

$$\mathrm{Fr} = \frac{V_{\mathrm{m}}^2}{g l_{\mathrm{m}}} = \frac{V_{\mathrm{f}}^2}{g l_{\mathrm{f}}}, \tag{1}$$

where g, V, and l are the gravitational acceleration ($\mathrm{m/s^2}$), velocity (m/s), and length (m), respectively; subscript m refers to the model-scale tunnel and f refers to the full-scale tunnel.

When choosing a geometric similarity ratio and gravitational acceleration similarity ratio as the basis for the similarity terms, the paper scale flow velocity (V), time (t), volume flux (Q), temperature (T), density (ρ), viscosity (u), and pressure (P) are described as [28, 29]

$$\begin{aligned}
\frac{V_{\mathrm{m}}}{V_{\mathrm{f}}} &= \left(\frac{L_{\mathrm{m}}}{L_{\mathrm{f}}}\right)^{1/2}, \\
\frac{t_{\mathrm{m}}}{t_{\mathrm{f}}} &= \left(\frac{L_{\mathrm{m}}}{L_{\mathrm{f}}}\right)^{1/2}, \\
\frac{Q_{\mathrm{m}}}{Q_{\mathrm{f}}} &= \left(\frac{L_{\mathrm{m}}}{L_{\mathrm{f}}}\right)^{5/2}, \\
\frac{T_{\mathrm{m}}}{T_{\mathrm{f}}} &= 1, \\
\frac{\rho_{\mathrm{m}}}{\rho_{\mathrm{f}}} &= 1, \\
\frac{u_{\mathrm{m}}}{u_{\mathrm{f}}} &= 1, \\
\frac{P_{\mathrm{m}}}{P_{\mathrm{f}}} &= \frac{L_{\mathrm{m}}}{L_{\mathrm{f}}},
\end{aligned} \tag{2}$$

where L is the geometric dimension and the subscript m is related to the model scale and index f is related to the full scale ($L_{\mathrm{m}}/L_{\mathrm{f}} = 1/10$ in this model test).

2.2. Determination of HRR. The heat release rate (HRR) is an important parameter in a fire experiment. Taking the requirements of the experiment and the worst-case scenario into consideration and referencing the result of project EUREKA EU 499 [30], the development rate of a train fire is determined as superfast growth, which means the value of the fire's increasing modulus $\alpha\,(\mathrm{kw \cdot s^{-2}})$ is 0.1876, and the value of the peak heat release rate is 15 MW. According to the principle of heat similarity, the HRR in a model tunnel is related to the HRR in a full-scale tunnel as the following equation indicates:

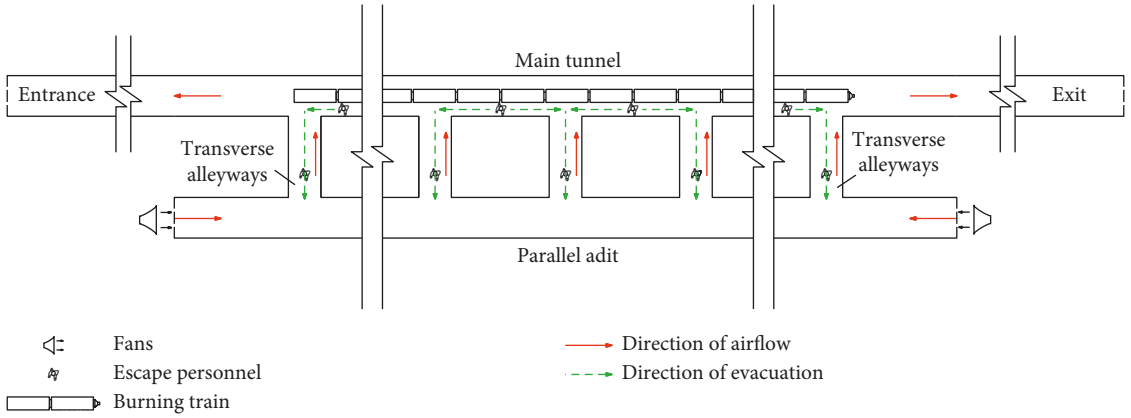

Figure 1: Schematic diagram of the rescue station.

$$\mathrm{HRR_m} = \left(\frac{L_\mathrm{m}}{L_\mathrm{f}}\right)^{5/2} \mathrm{HRR_f}, \tag{3}$$

where L is the length and subscript m refers to the model-scale tunnel and f refers to the full-scale tunnel.

Thus, $\mathrm{HRR_m}$ can be calculated by equation (3), and its value is 47.43 kW.

2.3. Experimental Configurations. Referring to the prototype rescue station in the Gaoligongshan Tunnel, a 1 : 10 reduced-scale model 60 m in length was built of concrete and bricks. The gradient of the model rescue station is −2.5%, which is the same as the prototype. The model consists of a main tunnel, a parallel adit, and nine permanently opened transverse alleyways. The geometry of the main tunnel is the same as that of the parallel adit. The width and height are 1.3 m and 0.962 m, respectively, which correspond to 13 m and 9.62 m, respectively, in the prototype. The width and height of each of the nine alleyways are 0.67 m and 0.615 m, respectively, which correspond to 6.7 m and 6.15 m, respectively, in the full-scale tunnel. The geometry of the model rescue station is shown in Figure 2. All cross sections of the model tunnel are horseshoe-shaped. In addition, the inner surface of the model rescue station was covered with cement mortar to guarantee the similarity of the friction coefficient between the model and the prototype. The constructed model rescue station is shown in Figure 3.

In the fire zone, which is five meters in all directions from the fire source position, the tunnel is made up of fire-resistant brickwork with fire-resistant mortar cement on the surface. These fireproof materials were used to decrease the potential effect of the high temperatures generated by fire. Two axial flow fans are mounted at the entrance and exit of the parallel adit, respectively. The flow velocity can be controlled by switching a valve to simulate different conditions. In this experiment, temperature fields in a superfast-growth fire without ventilation and with 0.7 m/s (2.21 m/s in the full-scale tunnel) inlet velocity in the parallel adit are tested.

A gasoline pool is chosen as the fire source. The gasoline pool fire is considered to have good reproducibility and less uncertainty [31], and its behavior conforms to superfast-growth fire well. The HRR is determined by the following equation:

$$Q = \eta m \Delta h, \tag{4}$$

where η is the combustion efficiency, with a value of 70%–80% for the gasoline pool; m is the mass loss rate that could be calculated by the relationship of mass and time; and Δh is the fuel heat value, which is about 46.6 MJ/kg for gasoline.

The HRR is regarded as one of the most important variables in a fire test, but it is very difficult to describe accurately. In order to make the HRR measurements as accurate as possible, the mass loss rate of the fire source was measured in a confined space similar in size to that in the experiment. The HRR is calculated based on equation (4), and the value is compared with the experiment result of the heat release rate of diesel oil pool fire [32] to verify its reliability. The evolution of the HRR as a function of time is shown in Figure 4.

The HRR value of a 25 cm×25 cm gasoline pool is about 53.08 kW. The corresponding HRR for the full-scale tunnel based on the site measurement of the mass loss rate is 16.79 MW. Three fire source positions (10 m, 30 m, and 50 m away from the entrance of the main tunnel) are set in the main tunnel to simulate the influence of different fire positions on the temperature field in a slope tunnel. Ignition holes are placed near every fire-source position for safety and convenience. The process of each experiment is to refuel gasoline to the pool, ignite the gasoline pool with a fire rod from the ignition hole, and then close the ignition hole; the test begins when the gasoline pool is ignited.

2.4. Measurement System. To study the temperature field of the main tunnel in different situations with different fire source positions and ventilation velocity, k-type thermocouples (temperature range from 0°C to 1300°C) are set in 45 sections to gather temperature data. The thermocouples are connected to the data collectors with compensation wires to reduce error, and the error of the temperature data is within 0.5%. The measurement sections are set every 1 m in the fire

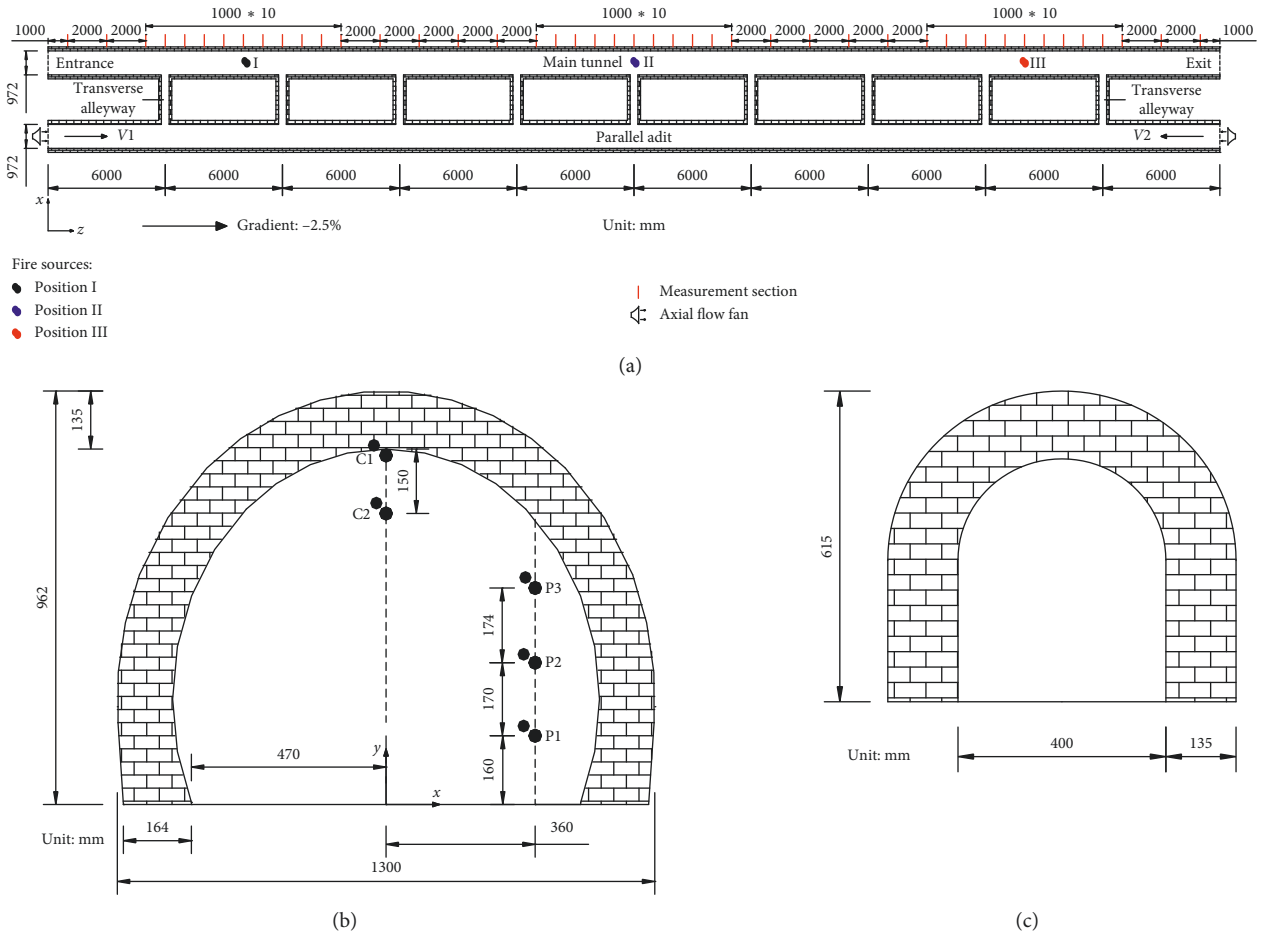

Figure 2: (a) Top view of the fire tunnel experiment with measurement sections. Cross sections of (b) the main tunnel with thermocouples and (c) the cross passage.

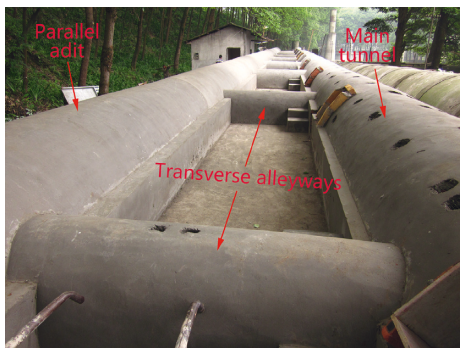

Figure 3: Actual model tunnel.

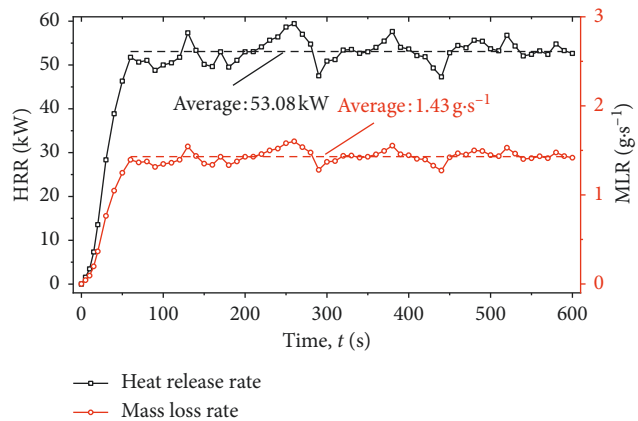

Figure 4: The evolution of the HRR as function of time.

zone and every 2 m in the nonfire zone. Two thermocouple trees are set in every measurement section, one beneath the ceiling and the other in the center of the evacuation platform. Considering the temperature beneath the ceiling is a key parameter in a tunnel fire model experiment and the maximum temperature usually appears at a distance from the ceiling, the thermocouple tree beneath the ceiling contains two thermocouples fixed at 0 cm and 15 cm below the ceiling. As the temperature field in the evacuation platform determines whether an evacuation can proceed smoothly, in this model experiment, the temperature field in the tunnel is tested. The thermocouple tree in the center of the evacuation platform contains three thermocouples at different positions: 16 cm, 33 cm, and 50.4 cm above the floor, as shown in Figure 2(b). Each data acquisition unit includes 32 output ports for measuring the temperature as well as an integrated operational amplifier, A/D converter, and microcontroller linked to a computer. The data collected

by the thermocouples are transmitted to a computer and processed by intelligent software. The data acquisition system was thoroughly tested and debugged before the formal model test and has been proved to be reliable. The layout of test instruments and the route of data transmission are shown in Figure 5.

2.5. Test Conditions. Twelve tunnel fire tests are performed, divided into free burn and ventilating by axial flow fans with different opening conditions in the parallel adit in different fire source positions (Table 1). Three different fire source positions are set at 10 m, 30 m, and 50 m from the entrance of the tunnel along the downhill direction, respectively, named position I, II, and III. Three methods of opening the axial flow fans are tested: the fan in the entrance, in the exit, and both fans opened. The velocity of the air in the model tunnel is 0.7 m/s consistently, corresponding to about 2.2 m/s in a full-scale tunnel.

3. Testing Results Analysis

3.1. Temperature Distribution along the Tunnel. Kurioka proposed an empirical formula to predict the maximum temperature of the smoke layer under a tunnel ceiling [7]. In the formula, the maximum temperature beneath the ceiling is related to the dimensionless heat release rate, the Froude number, the air velocity, and so on.

In a single tunnel, the hot air flows from one exit of the tunnel to the other. When the Kurioka formula is applied to a single tunnel without slope, the prediction fits the tested data well. In the rescue station, fresh air is forced to the main tunnel by the transverse alleyways from the parallel adit and flows to both exits of the tunnel; thus, the air flow is more complicated.

When the fire source is located at position III (i.e., 50 m away from the entrance) and all the fans in the parallel adit are closed (Test 9), the temperatures at the ceiling (Point C1) and at human eye-level height (1.6 m in the prototype) above the platform (Point P1) along the main tunnel are shown in Figures 6(a) and 6(b). The ceiling has the highest temperatures at the location of the fire: 91°C at 50 s, 342°C at 100s, 515°C at 300s, and 599°C at 600 s. The farther from the fire, the lower the temperature is at the ceiling. Near the fire, the temperature at the ceiling decreases dramatically. When the ceiling is about 3 m away from the fire, the temperature is less than 100°C at 600 s. Then, the temperature decreases gently with the increase in the distance to the fire. When the ceiling is about 10 m away from the fire source, the temperature decreases to less than 50°C at 600 s. Figure 6(a) also shows that the trend of temperature change on both sides of the fire (i.e., the entrance direction and the exit direction) is the same. As the light flue gas goes up and takes away a lot of heat, the temperature at the platform is much lower than that at the ceiling. For example, near the fire, the highest temperatures are at human height above the platform (Point P1): 80°C at 50 s, 93°C at 100 s, 165°C at 300 s, and 181°C at 600 s; these are much lower than the highest temperatures at the ceiling. Figure 6(b) also shows that the temperature distribution of point P1 along the main tunnel is different from that of point C1. On the right side (i.e., the exit direction), the temperature decreases dramatically to 18°C at 600 s when it is 2 m away from the fire location. On the other side, the entrance direction, the temperature decreases more gently. When it is 10 m away from the fire, the temperature at P1 is lower than 20°C. Hence, at human height above the platform, the left side of the fire has a higher temperature than the right side. This indicates that the light flue gas spreads more easily in the uphill direction.

When the fans in the parallel adit are opened, the temperature distribution in the main tunnel changes greatly, as shown in Figures 7(a) and 7(b) and Table 2. If only the fan at the entrance is opened (Test 10, $V1 = 0.7$ m/s and $V2 = 0$ m/s), the highest ceiling temperature at 600 s is 805°C, which is 34.4% more than the highest temperature (599°C) in the test with all the fans closed (Test 9, $V1 = 0$ m/s and $V2 = 0$ m/s). In this case, fresh air is forced into the main tunnel through the transverse alleyways. As the fresh air promotes the burning, the temperature near the location of the fire increases. The fresh air also blows the heated air to the exit of the tunnel (downstream) and causes the temperature on the left side of the fire (upstream) to decrease while the temperature on the other side (downstream) increases. If only the fan at the exit is opened (Test 11, $V1 = 0$ m/s and $V2 = 0.7$ m/s), the highest temperature is 783°C, 1 m away from the fire on the upstream side. Figure 7(a) also shows that the ceiling temperature on the left side of the fire (upstream) increases greatly. This indicates that the fresh air promotes the burning and diffusing upstream if only the fan at the exit is opened. When both fans are opened (Test 12, $V1 = 0.7$ m/s and $V2 = 0.7$ m/s), the ceiling temperature on both sides increases, and the highest temperature at 600 s is 644°C. Figure 7(b) shows that the temperature at human height above the platform increases too if the fans at the adit are opened. In Test 9, where $V1 = 0$ m/s and $V2 = 0$ m/s, the highest temperature is 181°C. In Tests 10, 11, and 12, the highest temperature at 600 s increases from 117%, 14.9%, and 148% to 392°C, 208°C, and 448°C, respectively, as shown in Table 2. The test results indicate that the temperature near the location of the fire increases a lot if the fans at the adit are opened because fresh air is forced into the main tunnel and promotes burning.

It can be seen from the experiments above that fresh air flows into the main tunnel through transverse alleyways as a result of the fans in the parallel adit, and it causes a change of the maximum temperature and temperature distribution along the tunnel. When a fan on only one side is opened, the supply of oxygen becomes more adequate, leading to a higher temperature at the ceiling. In terms of longitudinal temperature distribution at the ceiling, the temperature drops on the close-to-fan side but rises on the other side. When fans on both sides are opened, flow flux in the rescue station increases, and the high-temperature gas at the ceiling also spreads farther in the longitudinal direction. The maximum temperature and its distribution at human eye-level height above the platform seem to be more complex. As

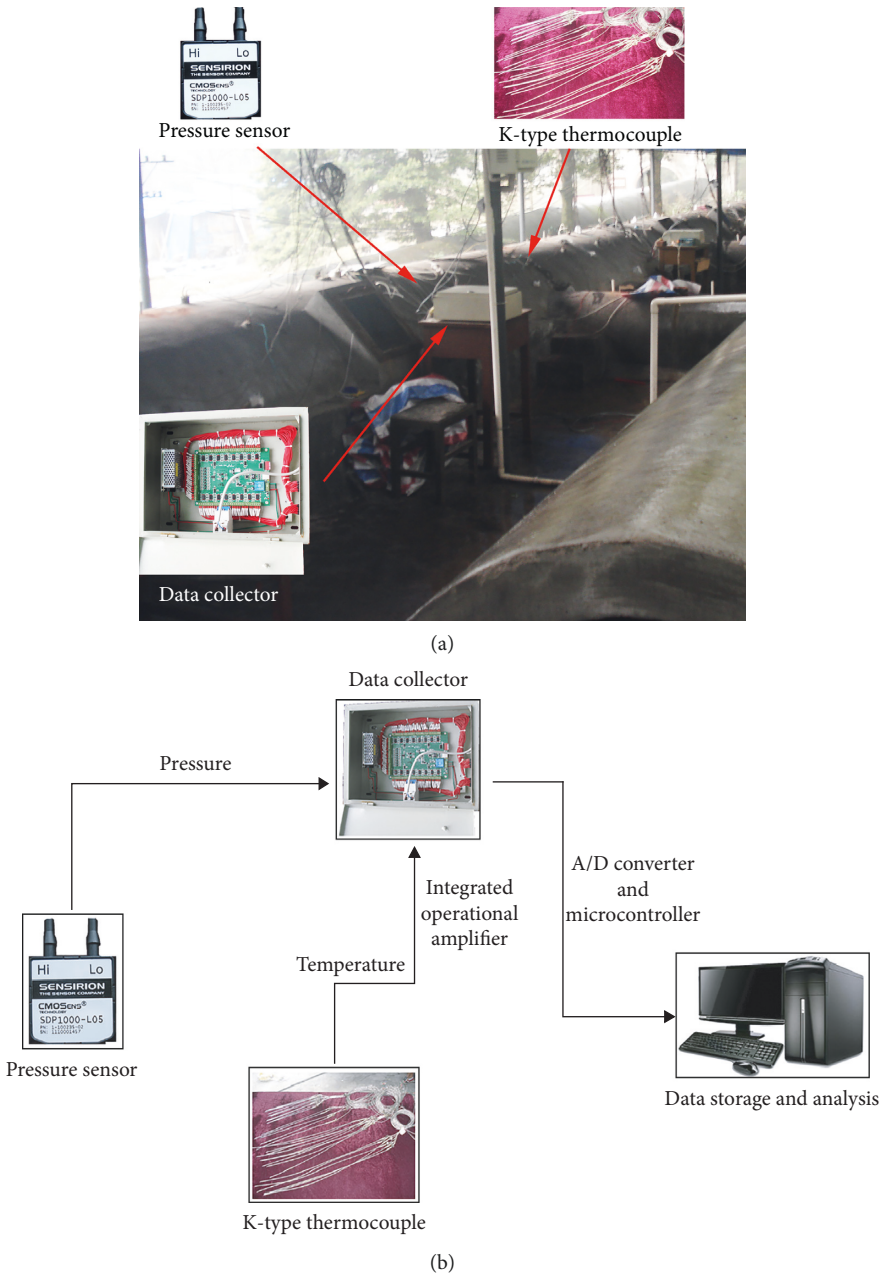

Figure 5: Measurement system: (a) layout and (b) diagram.

Table 1: Fire model test conditions.

Fire position: I			Fire position: II			Fire position: III		
Test no.	$V1$ (m/s)	$V2$ (m/s)	Test no.	$V1$ (m/s)	$V2$ (m/s)	Test no.	$V1$ (m/s)	$V2$ (m/s)
1	0	0	5	0	0	9	0	0
2	0.7	0	6	0.7	0	10	0.7	0
3	0	0.7	7	0	0.7	11	0	0.7
4	0.7	0.7	8	0.7	0.7	12	0.7	0.7

Note. $V1$, $V2$: air velocity of the fan at the entrance and exit of the parallel adit, m/s.

the measure points are set near the transverse alleyways, the fresh air can influence the temperature significantly. When the fan near the fire source is opened, the maximum temperature at human eye-level height decreases, and the diffusion distance of the high temperature is shortened. For the other two strategies of ventilation, the maximum

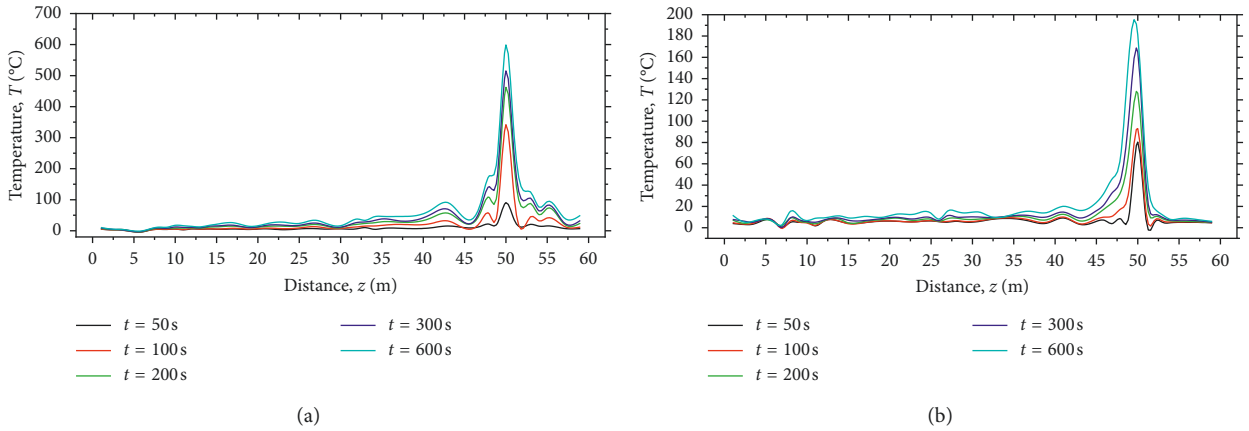

Figure 6: Temperature variation of the main tunnel (Test 9): (a) C1 and (b) P1.

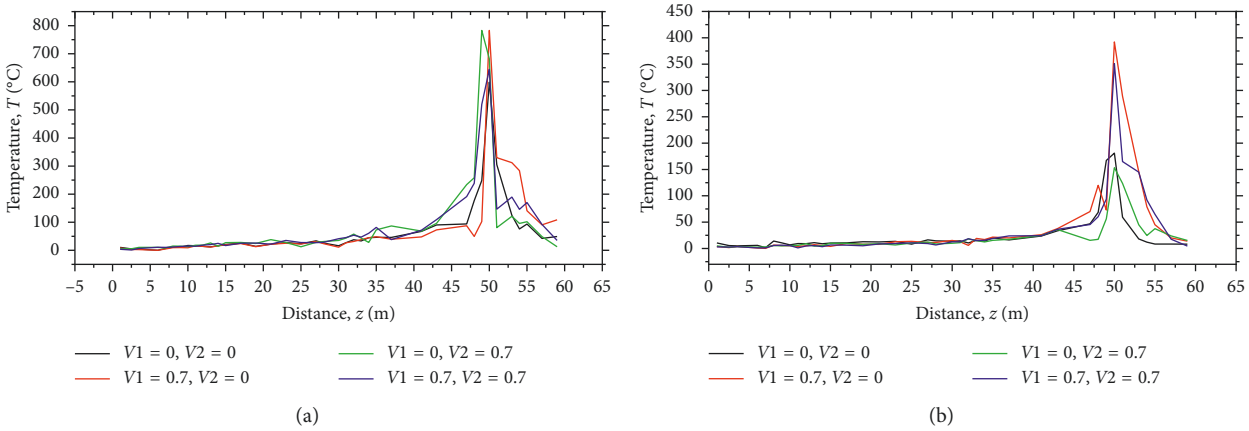

Figure 7: Temperature distribution with different ventilation. (a) C1. (b) P1.

Table 2: Maximum temperature at the ceiling (Point C1) and platform (Point P1).

Fire position: A			Fire position: B			Fire position: C		
Test no.	C1 (°C)	P1 (°C)	Test no.	C1 (°C)	P1 (°C)	Test no.	C1 (°C)	P1 (°C)
1	832	447	5	659	360	9	599	181
2	642	519	6	727	454	10	805	392
3	920	518	7	812	453	11	783	208
4	787	594	8	998	684	12	648	448

temperature increases and the high-temperature zone extends farther.

3.2. Time-Temperature Curves. Some time-temperature curves obtained based on full-scale or reduced-scale tests are used in specific applications such as RABT/ZTV (1985), HCM (1998), and EBA (2005) [26–28]. Engineers use these standardized time-temperature curves to design the support structure, disaster prevention methods, and rescue plans of a single tunnel. In the rescue station, because the air flow is more complicated, there is no universal guideline concerning how to choose the ideal curve in relation to the heat release rates, longitudinal ventilation velocity, or ceiling heights. The time-temperature curve reveals three stages of a tunnel fire: growing, stabilization, and decaying. In this test, temperatures in the growing and stabilization stages are measured.

Figure 8(a) shows the typical growth of the ceiling temperature (Point C1) when all the fans at the adit are closed (i.e., $V1 = 0$ m/s and $V2 = 0$ m/s). The time-temperature curve at the ceiling of the rescue station can be divided into four stages. Taking Test 5 (fire at position II) as an example, in the early stage, from test start to $t = 30$ s, the temperature grows gently from 20°C to 29°C at a rate of 0.3°C/s. In the rapid growth stage, from $t = 30$ s to $t = 120$ s, the temperature increases from 29°C to 390°C at a rate of 4.01°C/s. In the slow growth stage, from $t = 120$ s to $t = 270$ s, the temperature increases from 390°C to 599°C at a rate of 1.39°C/s. In the stabilization stage, from $t = 270$s to $t = 600$ s,

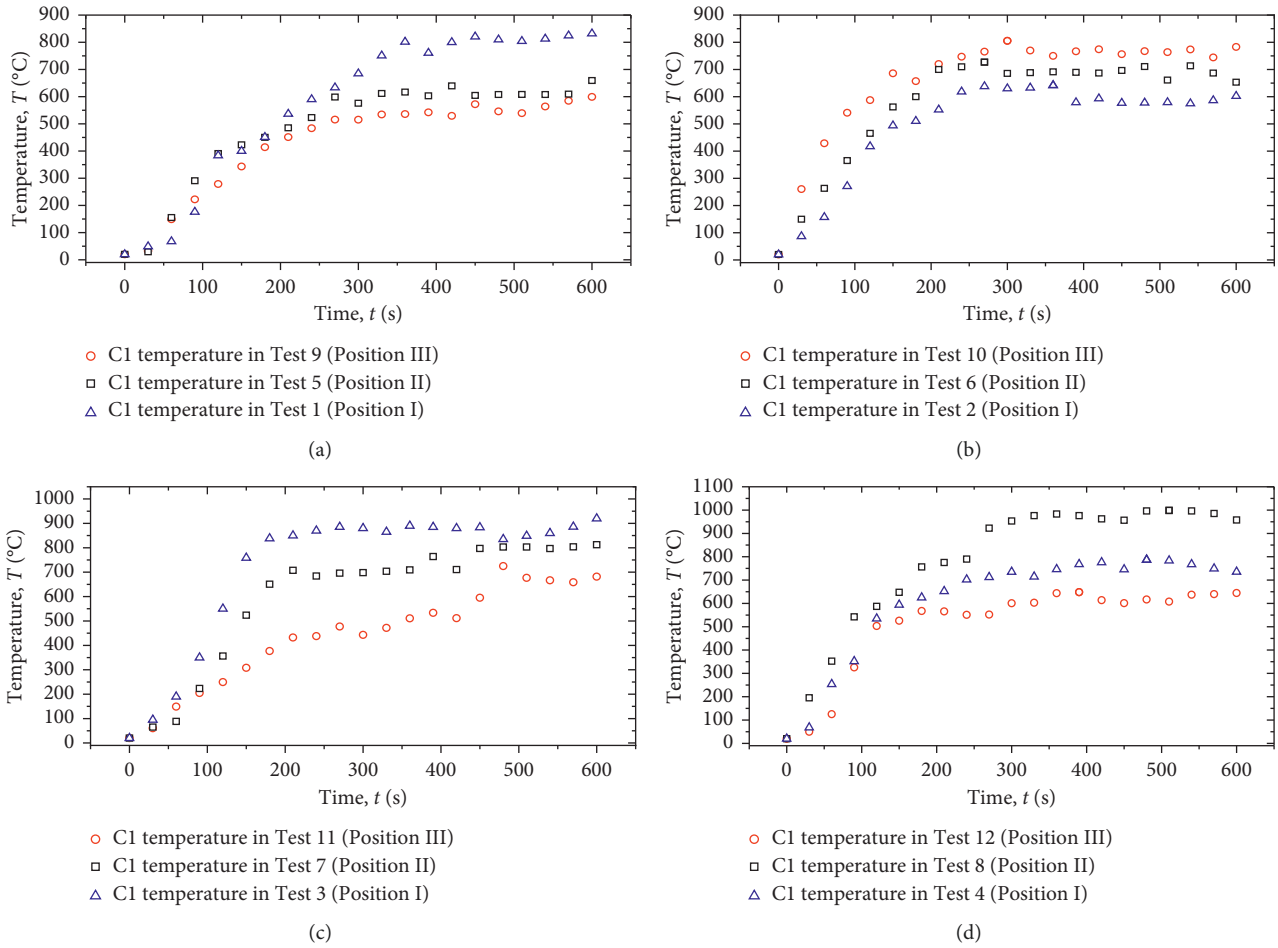

Figure 8: Temperature increase in the tunnel. (a) $V1 = 0$, $V2 = 0$. (b) $V1 = 0.7$, $V2 = 0$. (c) $V1 = 0$, $V2 = 0.7$. (d) $V1 = 0.7$, $V2 = 0.7$.

the temperature changes little. Figure 8(a) also shows that the fire position affects the ceiling temperature growth in the main tunnel. In Test 9, where the fire is at position III, the ceiling has the lowest temperature; in the rapid growth stage starting from $t = 30$ s to $t = 180$ s, the temperature increases at a rate of 2.55°C/s, which is lower than the growth rate in Test 5 where the fire is at position II. In Test 1 where the fire is at position I, the ceiling temperature has the longest slow growth stage, ranging from $t = 120$ s to 360 s at the rate of 1.75°C/s. The ceiling temperature in Test 1 is the highest at $t = 600$ s.

When the fan at the adit entrance is opened (i.e., $V1 = 0.7$ m/s and $V2 = 0$ m/s), the temperature at the ceiling increases a lot. In Test 10, where the fire is at position III, the early stage is too fast to be observed. In the rapid growth stage, approximately from the start of the test to $t = 150$ s, the temperature increases from 20°C to 686°C at a rate of 4.44°C/s. In the slow growth stage, from $t = 150$ s to $t = 300$ s, the temperature increases from 686°C to 805°C at a rate of 0.78°C/s. In the stabilization stage, from $t = 300$ s to $t = 600$ s, the temperature changes little. Figure 8(b) shows that the ceiling temperature growth in the main tunnel is greatly influenced by the wind blown in by the fan. The ceiling temperature in Test 2, where the fire is at position I, is the lowest; in the rapid growth stage starting from the beginning of the test to $t = 150$ s, the temperature increases at a rate of 3.16°C/s, which is the smallest rate of increase in Tests 2, 6, and 10. The chimney effect causes the hot flue gas to flow in the uphill direction. The wind blown in from the entrance weakens the influence of the chimney effect and prevents hot flue gas from flowing to the entrance so that the ceiling temperature in Test 10 is the highest. The chimney effect also prevents fresh air from flowing to the entrance and makes the fire in position I combust incompletely so that the ceiling temperature in Test 2 is the lowest.

Figure 8(c) shows the growth of the ceiling temperature when the exit fan at the adit is opened (i.e., $V1 = 0$ m/s and $V2 = 0.7$ m/s). Figure 8(c) shows that the C1 temperature in Test 3 (position I) is the highest while the C1 temperature in Test 11 (position III) is the lowest. Otherwise, the C1 temperature in Tests 11, 7, and 3 ($V1 = 0$ m/s, $V2 = 0.7$ m/s) are all higher than in Tests 9, 5, and 1 ($V1 = 0$ m/s, $V2 = 0$ m/s) because the wind blown in from the exit enhances the chimney effect and brings much more fresh air to the main tunnel and makes the fire burn faster and more violently.

Figure 8(d) shows the growth of the ceiling temperature when both fans at the adit are opened (i.e., $V1 = 0.7$ m/s and $V2 = 0.7$ m/s). In the early stage, the temperature increase in

Test 12 (position III) and Test 4 (position I) is much slower than that in Test 8 (position II). The C1 temperature in Test 8 ($V1 = 0.7$ m/s, $V2 = 0.7$ m/s) where the fire is at position II is the highest and much higher than that in Test 5 ($V1 = 0$ m/s, $V2 = 0$ m/s). The C1 temperatures in Tests 12 and 4 ($V1 = 0.7$ m/s, $V2 = 0.7$ m/s) are quite close to those in Tests 9 and 1 ($V1 = 0$ m/s, $V2 = 0$ m/s). This is because there is little influence from the chimney effect when the wind flows from both sides of the tunnel, and the hot flue gas gathers in the middle (position II).

Figure 9 shows some time-temperature curves at the height of the human eye-level (point P1). The features shown in Figure 9 are substantially the same as those in Figure 8. Figure 9(b) shows that ventilation in the same direction of the slope weakens the chimney effect. Figure 9(c) shows that ventilation in the same uphill direction enhances the chimney effect. Figure 9(d) shows that the wind flowing from both sides of the tunnel has little influence on the chimney effect but makes the hot flue gas gather in the middle.

At positions I, II, and III, opening the fan will make the fire burn more quickly, causing a faster increase in temperature in the early stage. For position I, opening the fan at the entrance ($V1 = 0.7$ m/s, $V2 = 0$ m/s) causes the combustion to slow down and the temperature decreases; opening the fan at the exit ($V1 = 0$ m/s, $V2 = 0.7$ m/s) or the fans at both sides ($V1 = 0.7$ m/s, $V2 = 0.7$ m/s) makes the fire burn more violently, resulting in temperature increases. For position II, opening either one or both fans makes the fire burn more quickly and more violently. Because the wind flowing from both sides makes the hot flue gas gather in the middle, the increase in temperature is the highest when the fans at both sides are opened: the temperature rises from 659°C to 998°C at point C1 and rises from 340°C to 684°C at point P1. For position III, opening either one or both fans also makes the fire burn more quickly and more violently. At point C1, the increase in temperature is the highest when the fan at the entrance is opened ($V1 = 0.7$ m/s, $V2 = 0$ m/s); the temperature rises from 599°C to 805°C; at point P1, the increase in temperature is the highest when the fans at both sides are opened ($V1 = 0.7$ m/s, $V2 = 0.7$ m/s); the temperature rises from 211°C to 448°C.

Based on the time-temperature curves at both ceiling and human eye-height level above the platform, it is clear that when the fire source is close to the fan in the parallel adit, the fresh air forced into the main tunnel through the transverse alleyways causes the measured temperature to decrease dramatically, compared with the condition in which all the fans are closed. By contrast, the temperature goes higher when the opened fan is far away from the fire source because the chimney effect causes some fresh air to flow into the tunnel from outside the tunnel, providing sufficient oxygen to make the fire burn even violently. Opening all the fans promotes air flow in the main tunnel and makes the combustion more complete so that the temperature goes much higher.

3.3. Temperature Distribution in the Main Tunnel. The temperature distribution in the platform is the key concern for rescue activities in a tunnel with a rescue station. The temperature at the human eye level decides the safety of the escape and thus needs to be studied scrupulously. Temperature field changes in the range of 5 m upstream and downstream of the fire source are studied because the fire source only affects the temperature field in the surrounding area.

Figure 10(a) shows the test temperature field in the center section of the platform, which is 360 mm away from the center of the cross section of the tunnel at 600s when all the fans at the adit are closed (i.e., $V1 = 0$ m/s and $V2 = 0$ m/s; Test 5). Because the hot flue gas rises to the ceiling, the higher the y direction, the higher the temperature. Due to the chimney effect, the temperature field is skewed toward the entrance direction. The temperature in the direction of the entrance is higher than that in the direction of the exit in general. The high-temperature zone ranges from 27.5–30.5 m in the z direction and 0.43–0.5 m in the y direction. The temperature, which is 263°C at point P3 at 26 m (z direction), is 55.4°C higher than that at 34 m. There is no temperature which is safe for personnel to escape in the direction of the entrance. By contrast, the temperature which is safe for personnel to escape is 3 m away from the fire source in the direction of the exit.

Figures 10(b)–10(d) show the test temperature fields in the center section of the platform at 600 s under ventilation. The opening of the entrance fan at the adit causes the wind to exit, resulting in the temperature field being skewed toward the exit direction and the rise of the maximum temperature. The wind flowing from the exit enhances the chimney effect and makes the temperature field of the platform skew obviously to the entrance direction. The temperature in the direction of the exit is much lower than that in the direction of the entrance in general. The temperature near the fire source will increase, and the high-temperature zone will connect through when all the fans in the adit are opened. Overall, the opening of the fan will bring more fresh air flow to the fire source so that the temperature increases.

When the fans are closed, the temperature field will skew toward the entrance direction due to the chimney effect. When the fans are opened, the temperature will increase because fresh air flows to the fire source and the temperature field will skew in the direction of wind flow.

4. Conclusions and Discussion

This paper reports the results of a model test of a fire in the rescue station of a railway tunnel. Specifically, the temperatures near the ceiling and platform of the main tunnel are tested in different conditions. Some conclusions from the tests are reported below.

The temperature distribution along the tunnel shows that fresh air that flowed to the main tunnel through the transverse alleyways by the fan at the adit promotes burning and makes the temperature increase. Without ventilation, the temperature distribution along the tunnel is stable and temperatures decrease gently. The time-temperature curves show that the temperature increase at the rescue station can be divided into four stages. Opening the fan will make the fire burn more quickly, causing a faster increase in

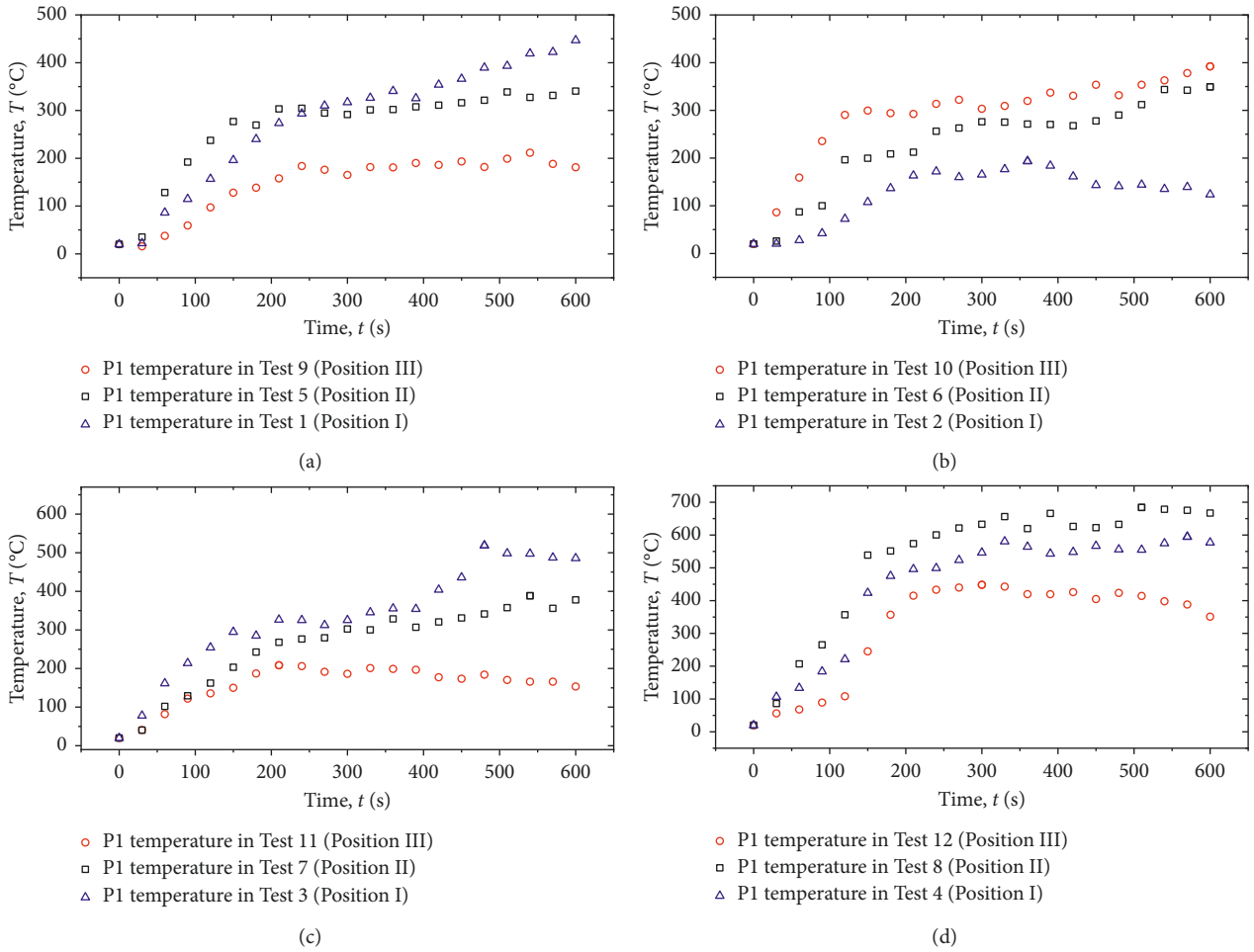

Figure 9: Temperature increase in the tunnel. (a) $V1 = 0$, $V2 = 0$. (b) $V1 = 0.7$, $V2 = 0$. (c) $V1 = 0$, $V2 = 0.7$. (d) $V1 = 0.7$, $V2 = 0.7$.

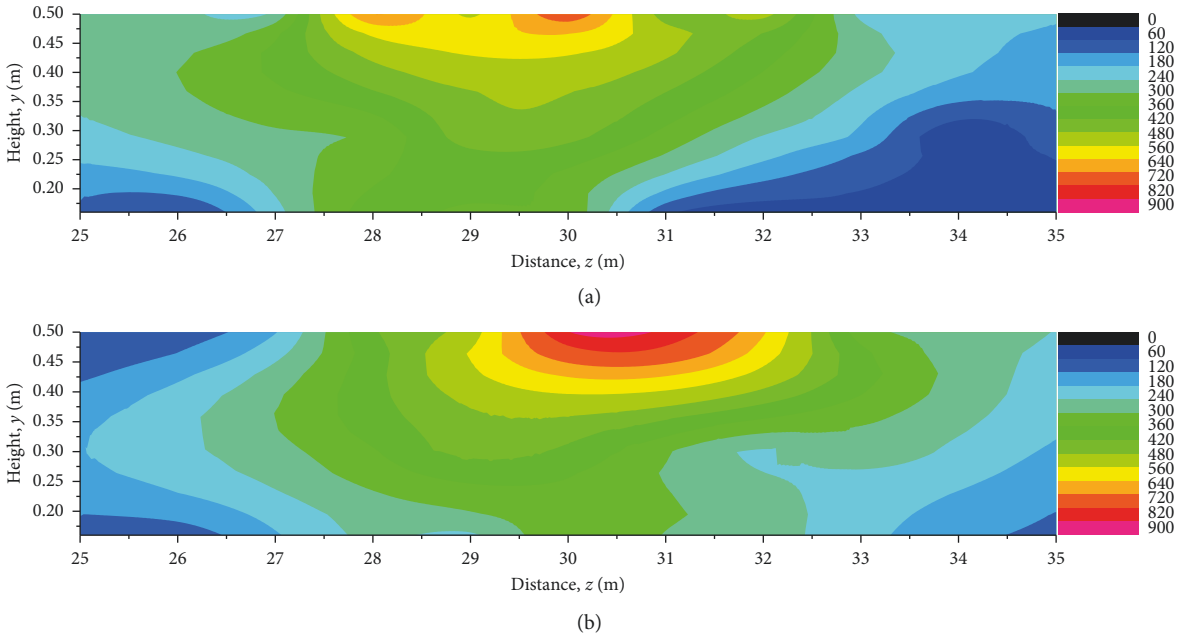

Figure 10: Continued.

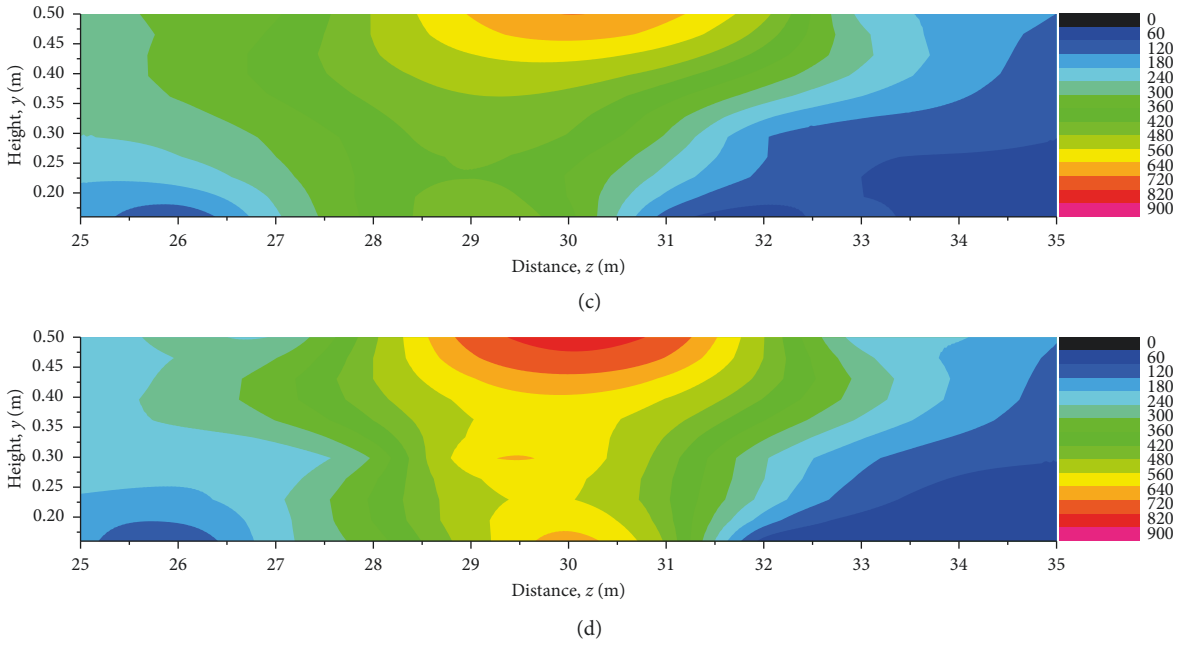

Figure 10: Cloud pictures of temperature distribution. (a) $V1 = 0$, $V2 = 0$. (b) $V1 = 0.7$, $V2 = 0$. (c) $V1 = 0$, $V2 = 0.7$. (d) $V1 = 0.7$, $V2 = 0.7$.

temperature in the early stage. The farther from the fan, the greater the temperature rise. Opening the fan which is far away from the fire source will cause a hazardous situation that will hinder the escape of personnel. Because of the chimney effect, the temperature is the lowest when the fire occurs at position III. From the temperature distribution in the main tunnel, the influence zone is within 5 m of the fire source. Due to the chimney effect, the temperature field will skew in the uphill direction, and the ventilation will influence the temperature field. The high-temperature zone will connect through when all the fans at the adit are opened, which is a dangerous condition for personnel escape. These findings provide a basis for designing safe evacuation and a foundation for further study of the temperature distribution in a tunnel with a rescue station.

Model tests are conducted under hypothetical ideal conditions. There are several limitations of this test. First, the natural wind near the entrance and exit would influence the velocity field in the tunnel. Second, the consistency of the HRR in these 12 tests are not strictly guaranteed, although the HRR of the fire source was measured. Third, the consistency of thermophysical properties in different materials is difficult to guarantee. The following items must be checked carefully before the test to make the test results reliable and repeatable: (1) ensure that the evolution of the HRR is consistent with that in a real tunnel; (2) avoid the interference of natural wind in the test; (3) ensure that the thermophysical properties of materials in the model are the same as those in a real tunnel.

Data Availability

The data used to support the findings of this study are available from the corresponding author upon request.

Conflicts of Interest

The authors declare that they have no conflicts of interest.

Acknowledgments

This paper was supported by the National Natural Science Foundation of China (No. 51678502) and the National Key R&D Plan of China (2016YFC0802201).

References

[1] A. Delisio, J. Zhao, and H. H. Einstein, "Analysis and prediction of TBM performance in blocky rock conditions at the Lötschberg Base Tunnel," *Tunnelling and Underground Space Technology*, vol. 33, pp. 131–142, 2013.

[2] A. Kitamura, "Technical development for the Seikan tunnel," *Tunnelling and Underground Space Technology*, vol. 1, no. 3, pp. 341–349, 1986.

[3] C. J. Kirkland, "The fire in the Channel tunnel," *Tunnelling and Underground Space Technology*, vol. 17, no. 2, pp. 129–132, 2002.

[4] H. Ehrbar, *Gotthard Base Tunnel, Switzerland. Experiences with different tunnelling methods*, in *Proceedings of 2° Congresso Brasileiro de Túneis e Estruturas Subterrâneas*, Sao Paulo, Brazil, 2008.

[5] F. Tarada, R. Bopp, S. Nyfeler et al., "Ventilation and risk control of the young dong rail tunnel in Korea," in *Proceedings of 1st International Conference on Major Tunnel and Infrastructure Projects*, Taiwan, 2000.

[6] D. H. Kim and W. H. Park, "Experiment by using reduced scale models for the fire safety of a rescue station in very long rail tunnel in Korea," *Tunnelling and Underground Space Technology*, vol. 21, no. 3-4, 2006.

[7] H. Kurioka, Y. Oka, H. Satoh, and O. Sugawa, "Fire properties in near field of square fire source with longitudinal ventilation

in tunnels," *Fire Safety Journal*, vol. 38, no. 4, pp. 319–340, 2003.

[8] Y. F. Wang, Y. L. Li, P. N. Yan, B. Zhang, J. C. Jiang, and L. Zhang, "Maximum temperature of smoke beneath ceiling in tunnel fire with vertical shafts," *Tunnelling and Underground Space Technology*, vol. 50, pp. 189–198, 2015.

[9] Y. Z. Li, B. Lei, and H. Ingason, "The maximum temperature of buoyancy-driven smoke flow beneath the ceiling in tunnel fires," *Fire Safety Journal*, vol. 46, no. 4, pp. 204–210, 2011.

[10] Y. Z. Li and H. Ingason, "The maximum ceiling gas temperature in a large tunnel fire," *Fire Safety Journal*, vol. 48, pp. 38–48, 2012.

[11] A. Kashef, Z. Yuan, and B. Lei, "Ceiling temperature distribution and smoke diffusion in tunnel fires with natural ventilation," *Fire Safety Journal*, vol. 62, pp. 249–255, 2013.

[12] F. Wang and M. Wang, "A computational study on effects of fire location on smoke movement in a road tunnel," *Tunnelling and Underground Space Technology*, vol. 51, pp. 405–413, 2016.

[13] F. Wang, M. Wang, R. Carvel, and Y. Wang, "Numerical study on fire smoke movement and control in curved road tunnels," *Tunnelling and Underground Space Technology*, vol. 67, pp. 1–7, 2017.

[14] F. Wang, M. Wang, and J. Huo, "The effects of the passive fire protection layer on the behavior of concrete tunnel linings: a field fire testing study," *Tunnelling and Underground Space Technology*, vol. 69, pp. 162–170, 2017.

[15] R. Ren, S. Xu, Z Ren et al., "Numerical investigation of particle concentration distribution characteristics in twin-tunnel complementary ventilation system," *Mathematical Problems in Engineering*, p. 13, 2018.

[16] R. Ren, H. Zhou, Z. Hu, S. He, and X. Wang, "Statistical analysis of fire accidents in Chinese highway tunnels 2000-2016," *Tunnelling and Underground Space Technology*, vol. 83, pp. 452–460, 2019.

[17] Z. Zhang, H. Zhang, Y. Tan, and H. Yang, "Natural wind utilization in the vertical shaft of a super-long highway tunnel and its energy saving effect," *Building and Environment*, vol. 145, pp. 140–152, 2018.

[18] Q. Yan, B. Li, Y. Zhang, J. Yan, and C. Zhang, "Numerical investigation of heat-insulating layers in a cold region tunnel, taking into account airflow and heat transfer," *Applied Sciences*, vol. 7, p. 679, 2017.

[19] L. H. Hu, R. Huo, W. Peng, W. K. Chow, and R. X. Yang, "On the maximum smoke temperature under the ceiling in tunnel fires," *Tunnelling and Underground Space Technology*, vol. 21, no. 6, pp. 650–655, 2006.

[20] J. Ji, C. G. Fan, W. Zhong, X. B. Shen, and J. H. Sun, "Experimental investigation on influence of different transverse fire locations on maximum smoke temperature under the tunnel ceiling," *International Journal of Heat and Mass Transfer*, vol. 55, no. 17, pp. 4817–4826, 2012.

[21] L. H. Hu, L. F. Chen, L. Wu, Y. F. Li, J. Y. Zhang, and N. Meng, "An experimental investigation and correlation on buoyant gas temperature below ceiling in a slopping tunnel fire," *Applied Thermal Engineering*, vol. 51, no. 1, pp. 246–254, 2013.

[22] Y. Fang, J. Fan, B. Kenneally, and M. Mooney, "Air flow behavior and gas dispersion in the recirculation ventilation system of a twin-tunnel construction," *Tunnelling and Underground Space Technology*, vol. 58, pp. 30–39, 2016.

[23] H. Nyman and H. Ingason, "Temperature stratification in tunnels," *Fire Safety Journal*, vol. 48, pp. 30–37, 2012.

[24] F. Ura, N. Kawabata, and F. Tanaka, "Characteristics of smoke extraction by natural ventilation during a fire in a shallow urban road tunnel with roof openings," *Fire Safety Journal*, vol. 67, pp. 96–106, 2014.

[25] W. K. Chow, Y. Gao, J. H. Zhao, J. F. Dang, and N. C. L. Chow, "A study on tilted tunnel fire under natural ventilation," *Fire Safety Journal*, vol. 81, pp. 44–57, 2016.

[26] Y. F. Wang, X. F. Sun, B. Li, T. Qin, S. Liu, and Y. Liu, "Small-scale experimental and theoretical analysis on maximum temperature beneath ceiling in tunnel fire with vertical shafts," *Applied Thermal Engineering*, vol. 114, pp. 537–544, 2017.

[27] J. G. Quintiere, "Scaling applications in fire research," *Fire Safety Journal*, vol. 15, no. 1, pp. 3–29, 1989.

[28] A. Li, Y. Zhang, J. Hu, and R. Gao, "Reduced-scale experimental study of the temperature field and smoke development of the bus bar corridor fire in the underground hydraulic machinery plant," *Tunnelling and Underground Space Technology*, vol. 41, pp. 95–103, 2014.

[29] Y. Zeng, K. Liu, X. Zhou, and L. Fan, "Tunnel temperature fields analysis under the couple effect of convection-conduction in cold regions," *Applied Thermal Engineering*, vol. 120, pp. 378–392, 2017.

[30] A. Haack, "Introduction to the Eureka-EU 499 Firetun project," in *Proceedings of International Conference on Fires in Tunnels*, pp. 3–19, Swedish National Testing and Research Institute, Borås, Sweden, 1994.

[31] O. R. Carvel, *Fire Size in Tunnels*, PhD Thesis, Division of Civil Engineering, School of the Built Environment, Heriot–Watt University, Edinburgh, UK, 2004.

[32] L. Yi, R. Huo, J. Y. Zhang et al., "Characteristics of heat release rate of diesel oil pool fire," *Journal of Combustion Science and Technology*, vol. 12, pp. 164–188, 2006, in Chinese.